

FEDSM-ICNMM2010-0, %

PHYSICALLY-BASED DROP SIZE DISTRIBUTION EVOLUTION OF ATOMIZED DROPS

Moussa Tembely *

Arthur Soucemarianadin

Laboratory of Geophysical and Industrial Fluid Flows,
University Joseph Fourier
53, 38041 Grenoble cedex, France
Email: moussa.tembely@ujf-grenoble.fr

Christian Lécot

Laboratory of Applied Mathematics,
University of Savoie
73376 Le Bourget-du-Lac Cedex, France

ABSTRACT

We report in this work the evolution of a physically-based drop size-distribution of atomized drops coupling the Maximum Entropy Formalism (MEF) and the Monte Carlo method. The atomization is performed using a Spray On Demand (SOD) print-head which exploits ultrasonic generation via a Faraday instability. The physically-based distribution is a result of the coupling of a MEF specific formulation and a general Gamma distribution. The prediction of the drop size distribution of the new device is performed. The dynamic model which prediction capability is fairly good is shown to be sensitive to operating conditions, design parameters and physico-chemical properties of the fluid. In order to achieve the drop size-distribution evolution, we solve the distribution equation, reformulated via the mass flow algorithm, using a convergent Monte Carlo Method able to predict coalescence of sprayed droplets.

NOMENCLATURE

a semi-major axis length of nozzle exit shape
 b semi-minor axis length of nozzle exit shape
 f_p vibrating frequency of the piezoceramic disc
 g gravity acceleration
 N total number of drops
 N_i number of drops in each class i
 ρ_f fluid density

μ_f fluid viscosity
 α_b nozzle tip beveled angle
 σ_f fluid surface tension
 θ_E equilibrium contact angle fluid/structure

INTRODUCTION

A general theory for predicting the drop-size distribution of spray remains an unsolved problem although some distributions (e.g Weibull and Rosin-Rammler distributions) follows from physically grounded percolation model of chaotic atomization [1]. It turns out at the end that the application of these theories leads ultimately to curve fitting. The generated droplets result from the dynamics of ligaments and their fragmentation [2]. The analysis of ligament fragmentation presuming to be consisted of sub-drops in different sub-layers have been performed in [3] where the ligament breakup is found to be very well represented by gamma distributions. All these models ultimately lead to distribution which are still to be fitted with experiment and do not account for the effect of the atomizer. The significant number of drops constituting a spray does not allow to precisely determine the diameter or velocity of each drop. There is a profuse literature discussing the prediction of representative drop diameter in spray. However, there are relatively few publications dealing with drop size distribution prediction. One of the possibility to describe quantitatively a spray is thus to adopt the tools of statistical analysis. Following [4], there are three methods for

*Address all correspondence to this author.

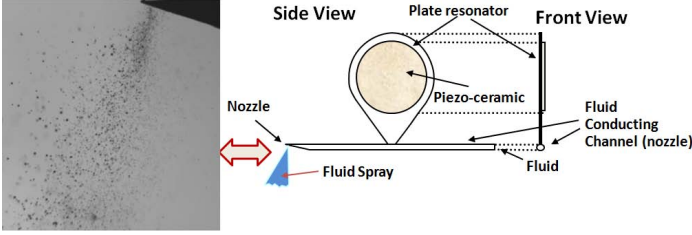


FIGURE 1. Spray On Demand print-head and visualization of the spray.

modeling drop size distribution: Empirical Method, Probability Function Method and the Maximum Entropy Formalism (MEF), the one adopted by us.

Despite of its enormous industrial application domain, spray modeling remains a challenge for computational methods and experimental measurements, when one wants to predict the drop size distribution. Droplet generation is an extremely complex process that cannot be precisely determined. Current approaches are either semi-empirical or need to be adjusted to each operating conditions. Based on the ultrasonic atomization via a Faraday instability of a new printhead termed as Spray On Demand(SOD) (see Fig. 1), we propose a physically-based drop size distribution, sensitive to operating conditions. Such an approach is necessary for obtaining a specific drop size distribution which may be required in some applications. Extended the MEF drop-size distribution for allowing a temporal evolution could be of great interest for initializing sophisticated CFD spray modeling codes. In traditional approaches precise drop size distribution is usually time-independent. Here we propose a modeling of the time-dependent drop size distribution of the MEF. We derive the distribution evolution equation and we use the Mass Flow Algorithm (MFA) for the simulation of the equation with a convergent Monte Carlo method.

NEW PHYSICALLY BASED MEF

Following [2] three interpretations have been attributed to the fragmentation process: (i) sequential cascade of breakups, this interpretation originated from Kolmogorov leads to the log-normal distribution; (ii) the aggregation scenarii which makes use of the Smoluchowski kinetic aggregation process leading to the fact that the drop-size distribution displays an exponential tail; (iii) finally the Maximum Entropy Formalism(MEF) which presentation by the author leads to a Poisson's distribution. It is worth adding to these interpretations the vision on the dynamics of ligaments, assuming to be made up of blobs of different layers [3].

Instead of being opposed, we show that these different interpretations could be complementary in some extent. From two visions of the MEF, we derive a new formulation for predicting

drop-size distribution. Our presentation will show that the MEF could lead to the same result as the ligament dynamics which are at the core of spray formation. The droplets coming from the breakup of these ligaments is explained by the way the poly-dispersity of the spray. Even though ultrasonics sprays are less disperse compared to other techniques [5].

In order to establish a physically-based approach, we propose a coupling of what we distinguish as 2 complementers formulations using MEF: we call them specific and general formulations. A specific formulation is based on conservation laws; this formulation is proven to give satisfactory results on the spray, the drawback being for spray small drops. Its advantage is that it takes into account the device operating parameters. Thus we propose to couple this approach with a general formulation leading to the three-parameter generalized gamma distribution. Indeed this distribution takes into account the general characteristics of a spray but does not take into account the unique feature of atomization device.

Specific formulation

This formulation, sensitive to SOD operating conditions, is based on spray conservation laws consisting of maximizing the following shannon entropy:

$$S(h_n(D)) = - \int_D h_n(D) \ln h_n(D) dD, \quad (1)$$

where the integration is performed on all the permissible states of the diameter $\int_D \equiv \int_{D_{min} \rightarrow 0}^{D_{max} \rightarrow \infty}$, with D_{min}, D_{max} respectively the spray drops minimum and maximum diameters.

Normalization constraint

$$\int_D h_n(D) dD = 1, \quad (2)$$

Conservation laws constraints

$$\int_D h_n(D) m_k(D) dD = H_k, \quad k = 1 \dots M. \quad (3)$$

The solution expresses in the continuous form as:

$$h_n(D) = \exp \left(\lambda_0^c - \sum_k \lambda_k^c m_k(D) \right), \quad (4)$$

where λ_k^c being Lagrange multipliers in continuous form.

Until recently this formulation of MEF were applied using conservation laws of mass, momentum or energy. Its predictive capability were quite satisfactory for the volume based distribution of the spray. In [7] is derived a distribution based only on the constraint of mass conservation, and the volume based distribution deduced gives good results for a pressure swirl atomizer. They applied the MEF not on the number-based fraction but on the volume-based fraction (which is not a probability as explained in [6]), and they end up by performing a change of variable to deduce the number based drop-size distribution. Other attempts have been made by exploiting this change of variable to end up with an acceptable number based distribution. In fact the problem of this specific formulation is to correctly predict the number based distribution specially for small droplets population which are mainly over predicted. To prevent this a "change of variable" has been used but this violates the MEF principle. Since then, with the introduction of the general approach [10], the previous formulation had some how been abandoned. Our approach here is to revisit the abandoned specific formulation and show its complementarity with the the general formulation approach and its consistency with the MEF principle. In fact how one can claim to predict a process as complicated as the atomization without using as much information as possible including the useful information of the specific formulation. Many aspects have an influence both the generation mechanism of the droplets, the atomizer itself as well as the fluid. In addition to these constraints, a practical approach for spray modeling is to use the minimum number of parameters in order to allow effective computation. Our approach aims to meet these requirements by coupling the presented specific formulation and the following general formulation.

General formulation

As previously mentioned all atomization processes can be seen as the break-up of a ligament. Therefore the ligament dynamics can be seen as general characteristic of a spray. Because of the random liquid motions in the ligament, the sub-drops of a layer overlap and merge. The solution of that evolution equation leads to the following gamma function or gamma number-based distribution [3]:

$$F_{Ln}(x = d/d_0) = \frac{\beta^\beta}{\Gamma(\beta)} x^{\beta-1} \exp[-\beta x], \quad (5)$$

where d_0 is the average blob or ligament diameter, and β the gamma distribution parameter.

Considering that the ligament population at the SOD nozzle is distributed as:

$$F_L(d_0) \approx \delta(d_0 - d_l) \quad (6)$$

In fact unlike the case for high speed jet ligament, ligament from the Faraday wave is less disperse and could be assume to have nearly the same dimension noted here d_l .

Therefore we can deduce the drop-size distribution of the spray ($F_{Sn}(D)$) using convolution of $F_{Ln}(D/d_0)$ and $F_L(d_0)$ as:

$$F_{Sn}(d) = \int F_L(d_0) F_{Ln}(d/d_0) \frac{d(d_0)}{d_l} = \frac{1}{d_l} F_{Ln}(d/d_l) \quad (7)$$

We finally deduce,

$$F_{Sn}(d) = \frac{1}{d_l} \frac{\beta^\beta}{\Gamma(\beta)} (d/d_l)^{\beta-1} \exp[-\beta(d/d_l)], \quad (8)$$

This gamma distribution could therefore represent the general description of a spray for example that of the SOD spray.

An alternative description of a spray leading to the gamma function as well could be made also by adopted the MEF formalism. This distribution is formulated with a single constraint on diameter expressing the definition of a mean drop diameter [10]:

$$\int_D D^q F_n(D) dD = D_{q0}^q. \quad (9)$$

where q and D_{q0} are two parameters of the distribution function $F_n(D)$.

To model the small drop limitation caused by the presence of surface tension forces, a diameter-class probability distribution, $g(D)$, continuously increasing with the diameter, is introduced [9]:

$$g(D) = \zeta D^{\alpha-1}, \quad (10)$$

where ζ is a constant and α is the third parameter of $F_n(D)$.

Giving birth is the three-parameter generalized distribution [9], [8],

$$F_n(D) = \frac{q}{\Gamma(\frac{\alpha}{q})} \left(\frac{\alpha}{q}\right)^{\frac{\alpha}{q}} \frac{D^{\alpha-1}}{D_{q0}^\alpha} \exp\left[-\frac{\alpha}{q} \left(\frac{D}{D_{q0}}\right)^q\right], \quad (11)$$

by maximizing the following relative entropy

$$S_D = - \int_D F_n(D) \ln \frac{F_n(D)}{\mu(D)} dD, \quad (12)$$

where $\mu(D) = g(D)^{\alpha-1}$, the probability of reaching a diameter D .

The specific approach allows determining some of the parameters of the general formulation as follows:

$$D_{q0} = \left\{ \int_D D^q h_n(D) dD \right\}^{1/q}, \quad (13)$$

$$H_k = \int_D m_k(D) F_n(D) dD, \quad k = 1 \dots M \quad (14)$$

The constraints as relevant as possible, reflecting the physics of atomization, should be chosen to determine the 3 parameters (D_{q0} , α , q) of the generalized gamma function in addition to Eqn. (13). Note that the specific formulation that we introduced was able (alone) to predict drop-size distribution, although that distribution poorly models distribution for small drops as previously mentioned [4].

APPLICATION TO THE SOD SPRAY

Predicting the drop size distribution of the new Spray On Demand(SOD) print-head is an important issue for device optimization and operation. In the following we apply the previous approach to the SOD with the details of the specific formulation constraints on mass and energy.

Mass conservation

Let M_s be the mass of fluid accumulated at nozzle tip and which is ejected after an excitation time or operation of the SOD and which will break-up into droplets (Fig. 2). It corresponds to the total mass of fluid bursting at the nozzle tip interface due to Faraday instability, a direct consequence of the acceleration. The mass M_s of fluid is a reference quantity on which we will make our argument on mass and energy conservation. Therefore its precise value is not an issue. We assume M_s to be atomized into spray droplets with the drop diameter space divided into n_c classes of constant width ΔD . Let N_i be the number of drops in each class, it is possible to build the histogram of the frequency of occurrences of a given class. We denote $p_i = N_i/N$ the frequency of the number-based probability distribution whereas the

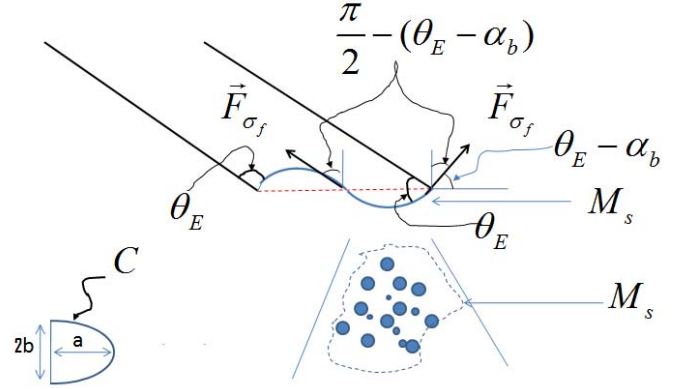


FIGURE 2. Drop hanging at the nozzle and atomization modeling.

continuous version is a probability density function, referred to as the number-based drop-size distribution with notation $h_n(D)$. We deduce the constraint upon mass conservation as :

$$\sum_{i=1}^{n_c} p_i d_i^3 = 1 \quad \text{with} \quad d_i = \frac{D_i}{D_{30}}. \quad (15)$$

Energy Conservation

The instability leading to droplet formation can be viewed as the conversion of the surface energy, $E_{surface}$, and fluid film kinetic energy, E_{vib} , of the hanging drop (of mass M_s) at the nozzle exit, to the droplets surface energy, $E_{droplets}$ generated in addition to the dissipation due to fluid viscosity¹:

$$\sum_{i=1}^{n_c} p_i d_i^2 = \frac{D_{30}}{D_c}. \quad (16)$$

where D_c corresponds to a characteristic diameter of the process equivalent to the Sauter Mean Diameter D_{32} for energy constraint. In fact, we can rewrite the energy constraint as:

$$\sum_{i=1}^{n_c} p_i D_i^2 = \frac{\sum_{i=1}^{n_c} p_i D_i^2 \cdot \sum_{i=1}^{n_c} p_i D_i^3}{\sum_{i=1}^{n_c} p_i D_i^3} = \frac{D_{30}^3}{D_{32}}, \quad (17)$$

and deducing by identification that $D_c \equiv D_{32}$.

¹Gravitational potential energy and dissipation are neglected.

From the energy constraint, we can establish a relationship for estimating the Sauter Mean Diameter of the SOD depending on the physical mechanical and operating conditions of the print-head [17]:

$$D_{32} = \left[\rho_f \frac{\pi}{6} \left(\frac{abg}{2\sigma_f \sin(\theta_E - \alpha_b)C} + \frac{f_p^2}{\sigma_f} \left[\frac{1}{4} \left(\frac{\mu_f \sigma_f}{\rho_f^2 f_p^3} \right)^{2/5} + B^2 \right] \right) \right]^{-1}, \quad (18)$$

where B corresponds to the vibrating amplitude of the SOD nozzle depending on the tube properties.

From the unstable wavelength, we can express the volume mean diameter (D_{30}) with a proportional constant ζ_1 as [17]:

$$D_{30} = \zeta_1 \left(\frac{\mu_f \sigma_f}{\rho_f^2 f_p^3} \right)^{1/5}. \quad (19)$$

where ζ_1 could be determined using experimental measurement.

Solving the MEF system leads to :

$$p_i = \exp(-\lambda_0 - \lambda_1 d_i^2 - \lambda_2 d_i^3). \quad (20)$$

The following minimization allows determining the Lagrange multipliers to fully compute Eqn. (20),

$$\min \left\{ \ln \left[\sum_{i=1}^{n_c} \exp(-\lambda_1 (d_i^2 - k) - \lambda_2 (d_i^3 - 1)) \right] \right\} \text{ gives } \lambda_1, \lambda_2, \quad (21)$$

and the multiplier λ_0 is given from normalization constraint, i.e $\sum_{i=1}^{n_c} p_i = 1$, by

$$\lambda_0 = \ln \left[\sum_{i=1}^{n_c} \exp(-\lambda_1 d_i^2 - \lambda_2 d_i^3) \right]. \quad (22)$$

Hence, as previously seen the number-based drop-size distribution of the specific formulation expresses as:

$$h_n(D_i) = \frac{p_i}{\Delta D}. \quad (23)$$

Predicting drop size distribution

The specific approach is limited by the fact that $h_n(D)$ generally over predicts small droplets population [4]. While the generalized gamma function found to be identical to a Nukiyama-Tanasawa distribution [8] is in good agreement with most experimental measurements both for number-based $f_n(D)$ and volume-based $f_v(D)$ distributions [26]. For our modeling we thus apply our approach for the general formulation using the three-parameter generalized gamma distribution:

$$F_n(D) = \frac{q}{\Gamma\left(\frac{\alpha}{q}\right)} \left(\frac{\alpha}{q}\right)^{\frac{\alpha}{q}} \frac{D^{\alpha-1}}{D_{q0}^{\alpha}} \exp\left[-\frac{\alpha}{q} \left(\frac{D}{D_{q0}}\right)^q\right]. \quad (24)$$

For the new approach we propose, we use the physically-based approach of the specific formulation to compute the diameter D_{q0} and parameter α respectively using the following relationship,

$$D_{q0} = \left\{ \int_D D^q h_n(D) dD \right\}^{1/q} \text{ and } D_{32} = \frac{\int_D D^3 F_n(D) dD}{\int_D D^2 F_n(D) dD}, \quad (25)$$

where $h_n(D)$ is given using Eqn. (23).

We can express the Sauter Mean Diameter as:

$$D_{32} = \frac{\alpha^{-\frac{1}{q}} D_{q0} q^{\frac{1}{q}} \Gamma\left(\frac{3+\alpha}{q}\right)}{\Gamma\left(\frac{2+\alpha}{q}\right)}. \quad (26)$$

The parameter q is fixed by using experimental measurement; this parameter is mainly sensitive to atomization process [26], it has a unique value for a given atomizer. Therefore it is assumed for our modeling as a constant. This approach allows a dynamic drop size distribution in contrast with the classical approach where the parameters have to be adjusted for each operating conditions. The coupling of the previous physical methods allow our model to be sensitive to physical mechanical and operating conditions of the device.

Experimental measurements: shadow imaging technique setup

The spray is illuminated in a backlight configuration by a non-coherent short flash source (15 ns in duration) to freeze the movement of the droplets on the images. The detector of the monochrome camera is composed of 1 008 x 1 018 square pixels of 9 μm side. An objective composed of 2 lenses ($f_{oc1}=300\text{mm}$ and $f_{oc2}=100\text{mm}$) and of lateral magnification $G = 3.7$ is used to obtain high-resolution images. The field of view is 2.44 mm x

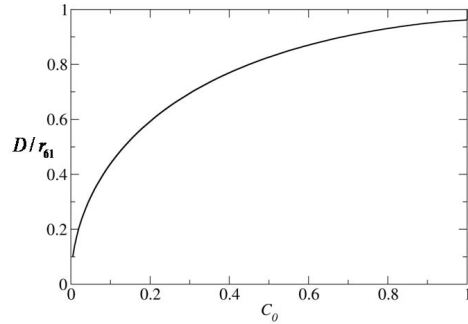


FIGURE 3. Curve for droplet diameter evaluation.

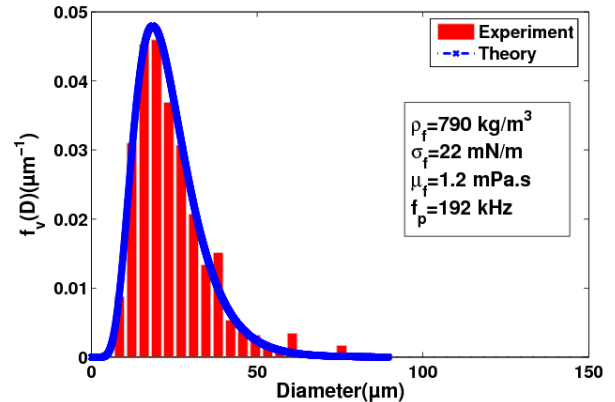


FIGURE 4. Physical model drop size distribution validation of a new Spray On Demand print-head.

2.46 mm and the resolution is 4130 pixels/cm. A 3-step image-processing program developed in C++ is applied to the images [19]. The first step consists of a normalization of the images to enhance the contrast of the images and to correct non-uniform background illumination. In a second step, images are binarized using two thresholding techniques. A classical threshold based on the range of grey levels in the image and a threshold based on the wavelet transform (in order to detect the out-of-focus droplets). This technique allows detection of local grey level variations of low contrast images in order to localize the maximum number of droplets and to associate to each of them a surrounding mask. Then each droplet is separated from its neighbors within the mask in order to be individually analyzed. The sub-pixel contour of the droplet is computed. The diameter of each droplet is defined as the equivalent surface radius (r_{61}) of the binarized image of the droplet at a level equal to 61% of the local grey level amplitude. An imaging model has been developed in order to estimate correctly the diameter [20]. The ratio of the real diameter (D) to the equivalent surface radius (r_{61}) is directly related to the contrast (C_0) of the droplets, as shown in Fig. 3. This curve is used to estimate the real diameter of the drops. Moreover, the level of out-of-focus of each droplet is determined in order to sort the droplets relatively to their spatial position from the focus plane. This is achieved through the calibration of the Point Spread Function (PSF) of the optical setup. Indeed, the PSF gives information on the out of-focus of droplets [20]. Droplets of low contrast (< 0.1) and of high level of out-of-focus (PSF > 0.1 mm) are so rejected.

Model constants determination

We experimentally determine the drop-size distribution of our new print-head using high speed camera and imaging post-processing treatment. An adjustment is made in order to determine the 2 constants of the model. Once these parameters are determined, the model can predict the behavior of the device when physical and operating conditions are changed. From comparison with experimental results in Fig. 4, and using fitting tools,

we deduce the 2 constants of our model (see Table 1). It is to be noted that the model takes into account the different physical parameters such as the mean diameters, the micro-channel motion, and also the voltage applied to the PZA and many other parameters required for SOD operation [11, 12].

ζ_1	q
2.98	0.21

TABLE 1. The constants of the model.

Design parameters: Model Prediction Capability

Our main goal is to test the model ability to predict qualitatively the drop-size distribution so that to have tools for the SOD optimization. For a quantitative study further measurements would be necessary which will require a reliable SOD, with a qualitative study performed here. The device, described in this paper together with the proposed modeling has been used in a host of innovative microfluidic applications such as metalization and fuel cell manufacture [17]. The results reported in Fig. 5 are predictions of the model with respect to various operating conditions and physical properties of the fluid (see Fig. 5(a)), by the way the curves show the more the surface tension is high the more disperse is the drop size distribution. A decrease of the surface tension leads to a finer spray droplets where the distribution shifts toward the small droplets population with an increase of the main peak height. This trends is in good agreement with the capillary instability, assuming the unstable wavelength is related to the spray droplet size [23]. These different results are in

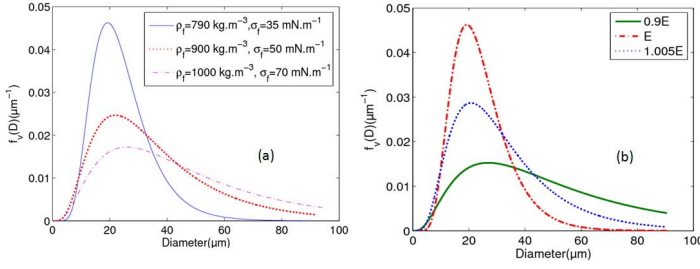


FIGURE 5. Prediction of Physical model drop size distribution (a) fluid properties (b) design constant with the tube Young Modulus $E=200$ MPa.

good agreement with experimental results [25] for ultrasonic atomizer. The model capability is also tested on design parameter as well in Fig. 5(b) through the SOD nozzle Young's modulus .

DROP SIZE-DISTRIBUTION EVOLUTION EQUATION

We assume that the real physical drop size distribution varies with time, for example under the effect of coalescence and breakup. The MEF traditionally used ignores the temporal evolution on the distribution. In the following section we undertake an analysis combining the physically based-MEF approach [11, 12] with the balance population method allowing the evolution of the drop size distribution.

The evolution of the distribution function is governed by a Boltzmann-type equation [13]. We focus on the effect of coalescence and we neglect the breakup, evaporation and nucleation phenomena. Using the drop size distribution in a formulation where it depends only on time t , and volume V (or diameter D), the balance population equation for the distribution $f_n(V, t)$ can be expressed as:

$$\begin{aligned} & \frac{\partial [N(t)f_n(V, t)]}{\partial t} \\ &= \frac{1}{2} \int_{V_{min}}^V K_c(V - V', V') N(t) f_n(V - V', t) N(t) f_n(V', t) dV' \\ & \quad - N(t) f_n(V, t) \int_{V_{min}}^{V_{max}} K_c(V, V') N(t) f_n(V', t) dV', \quad (27) \end{aligned}$$

where $N(t)$ is the total number of particles at time t . The right hand side (rhs) term represents source and sink effects due to coalescence. In this work we consider only binary interactions where broken droplets split into two smaller ones and where two droplets can coalesce to form a bigger one (before impacting on the substrate).

The probability of finding a drop with a volume comprised between V_i and $V_i + \Delta V$ is the same as the probability of finding a drop with a diameter comprised between D_i and $D_i + \Delta D$. The change between the volume and diameter formulation is carried out using the following relationship

$$f_n(D) dD = f_n(V) dV. \quad (28)$$

Then we deduce:

$$f_n(V) = \frac{2}{\pi D^2} f_n(D), \quad (29)$$

$f_n(V, t)$ being the number-based drop-volume distribution to be determined by our analysis. The equation relating the number $f_n(D)$ and volume $f_v(D)$ based drop size distributions is given by:

$$f_v(D) = \left(\frac{D}{D_{30}}\right)^3 f_n(D). \quad (30)$$

The total number of droplets in the range $V + dV$ at time t expresses as:

$$n(V, t) = N(t) f_n(V, t) dV. \quad (31)$$

Then we deduce the discrete form of the equation verified by the average number of droplets in class i , $n(V_i, t)$ as :

$$\begin{aligned} \frac{\partial n(i, t)}{\partial t} &= \frac{1}{2} \sum_{j=1}^i k_c(i - j, j) n(i - j, t) n(j, t) \\ & \quad - n(i, t) \sum_{j=1}^{n_c} k_c(i, j) n(j, t), \quad (32) \end{aligned}$$

where we set $k_c(i, j) = K_c(V_i, V_j)$ and $n(V_i, t) = n(i, t)$.

Coalescence Kernel Determination

One difficulty in our approach is to correctly write down the kernel, expressing the coalescence of drops. We express the coalescence kernel as the product of the coalescence efficiency (L_e) and the collision frequency (H_f),

$$K_c(V, V) = K_a L_e(V, V') H_f(V, V'), \quad (33)$$

where we have introduced K_a an adjustable constant depending on the situation.

Coalescence efficiency

Following [14] we assume that the coalescence efficiency could be expressed as :

$$L_e(V, V') = \exp[-t_{coal}(V, V')/t_{cont}(V, V')], \quad (34)$$

where $t_{coal}(V, V')$, $t_{cont}(V, V')$ respectively are average coalescence time and contact time of particles of volume V and V' . The time required for coalescence could be estimated [15] using

$$t_{coal}(V, V') = C_1 \left(\frac{R_{V, V'}^3 \rho_f}{\sigma_f} \right)^{1/2}. \quad (35)$$

where C_1 is a constant close to 2; σ_f surface tension, ρ_f is the density. $R_{V, V'}$ is the equivalent radius of the radii of coalescing drops and is defined as :

$$R_{V, V'} = \left(\frac{1}{D(V)} + \frac{1}{D(V')} \right)^{-1} \quad (36)$$

with $D = (6V/\pi)^{1/3}$.

The contact time is estimated in [16] for flowing fluid and the contribution due to relative velocities between bubbles and assumed here for droplets:

$$t_{cont}(V, V') = \frac{D(V) + D(V')}{2u_r(V, V')}. \quad (37)$$

Here we have neglected the turbulence effect. We denote $\vec{u}_r(V, V')$ the relative velocity between drops of volumes V and V' . The determination of this relative velocity is performed as follows. The relative velocity can be expressed by estimating the terminal velocity of falling particles. We assume in our model that coalescence happens only after this regime is reached, which is reasonable since the momentum velocity response time ($\approx D^2 \rho_a / \mu_a$) is small, considering the micro-metric size of the spray droplets.

From Newton's second law of falling particles, once the terminal velocity is reached, we have:

$$R_{ea}^2 C_D = \frac{4}{3} G_a, \quad (38)$$

where $R_{ea} = \rho_a V_l D / \mu_a$ and $G_a = D^3 g (\rho_f - \rho_a) \rho_a / \mu_a^2$ are respectively the Reynolds and Galileo (or Archimedes) numbers; ρ_f , μ_f , (ρ_a, μ_a) are respectively the density and viscosity of fluid (resp. of the surrounding gas, i.e, air); g is the gravity acceleration; V_l is the terminal velocity to be determined.

For a spherical fluid particle at low Reynolds number, the Stokes flow analysis leads to the Hadamard-Rybczynski drag law in which the shear stress on the surface induces an internal motion. The drag coefficient expresses :

$$C_D = \frac{8}{R_{ea}} \frac{2 + 3\kappa}{1 + \kappa}, \quad (39)$$

with the viscosity ratio $\kappa = \mu_f / \mu_a$. This result could be compared to that for a solid particle, where $C_D = 24/R_{ea}$.

Combining Eqn. (38) and Eqn. (39) we deduce the terminal velocity $V_l(V)$ (for a particle of volume V) i.e the relative velocity between the fluid particle and air.

$$V_l = \frac{1}{6} \frac{1 + \kappa}{2 + 3\kappa} \frac{D^2 g}{\mu_a} (\rho_f - \rho_a). \quad (40)$$

If we assume that spray droplets reach velocities close to their terminal velocity before coalescing with arbitrary angles (β), the relative velocity between two particles could be expressed as:

$$u_r^2 = \left\| V_l(V) - V_l(V') \right\|^2 = V_l(V)^2 + V_l(V')^2 - 2V_l(V)V_l(V') \cos \beta. \quad (41)$$

Then we take the average velocity from velocity directions 0 to $\pi/2$, leading to $\langle \cos \beta \rangle_{0, \pi/2} \approx 2/\pi$ with $\langle \bullet \rangle_{0, \Theta} = (1/\Theta) \int_0^\Theta \bullet dx$.

Collision frequency

In order to assess the rate of collision or the collision frequency, we consider two particles of diameters D and D' . When we consider the frame related to particle D , then particle D' evolves with the relative velocity $\vec{u}_r(V, V')$. The necessary conditions to assure the collision between these particles are :

- Particle (D) is located in a cylinder which axis is parallel to $\vec{u}_r(V, V')$ with a diameter of $D + D'$, which by the way defines the cross-section $S_c = \pi(D/2 + D'/2)^2$;

- To have a collision between times t and $t + dt$, it is necessary that the distance between the centers of the two particles, measured parallel to $\vec{u}_r(V, V')$, is less than or equal to $u_r(V, V')dt$. In other words, the particle (D) must be located in the collision volume i.e the volume of cylindrical section S_c and length $u_r(V, V')dt$. Therefore we deduce that the number of collisions of particles of type (D) with a particle of type (D') during the time interval dt is $n_p S_c u_r(V, V')dt$. If we extend this result to all the particles of type (D'), the collision frequency could be expressed in the following form:

$$H_f(V, V') = S_c n_p n'_p u_r(V, V') \\ = \pi n_p n'_p V_T (D/2 + D'/2)^2 u_r(V, V'), \quad (42)$$

where n_p, n'_p are the numbers of particles per unit volume of size respectively V, V' ; S_c being the collision cross-section of the two droplets. We approximate $n_p n'_p \approx (n(V, t = 0))/V_T (n(V', t = 0))/V_T$ using Eqn. (31). With $V_T = V_{spray}/\alpha_V$, α_V is a constant, expressing the spray volume fraction (or dispersed phase volume fraction) and V_{spray} the total volume of the spray droplets, see the following subsection.

Combining Eqn. (33), Eqn. (34) and Eqn. (42), we obtain the coalescence kernel:

$$K_c(V, V') \approx \tilde{K}_a C_N (D(V)/2 + D'(V')/2)^2 \\ V_{spray} u_r(V, V') \exp[-t_{coal}(V, V')/t_{cont}(V, V')]. \quad (43)$$

where we set $C_N = \pi(n(V, t = 0))(n(V', t = 0))/V_{spray}^2$, and the constant of our model $\tilde{K}_a = K_a \alpha_V$.

We easily verify the following properties of the kernel : $k_c(i, j) = k_c(j, i) \geq 0$. Eqn. (43) can also be seen as a general form for a coalescence kernel which takes into account mutual particle cross section, relative velocity and a particle coalescence efficiency.

REFORMULATION OF THE DROP-SIZE DISTRIBUTION EQUATION

The method of moments and the size-binning method do not describe the precise behavior of the drop size distribution. Monte-Carlo method seems to be a more advantageous choice and describes with precision the evolution of the drop size distribution [18, 21, 22]. In order to carry out a precise numerical analysis, we reformulate the problem in terms of mass conservation and then develop a Mass Flow Algorithm (MFA).

Multiplying Eqn. (32) by the volume V_i and summing over all i , leads us to the mass conservation equation (assuming that the density of the fluid (ρ_f) is constant):

$$\sum_{i=1}^{n_c} V_i n(i, t) = \sum_{i=1}^{n_c} M(i, t) = \sum_{i=1}^{n_c} M(i, 0) = \frac{m_0}{\rho_f} = V_{spray}. \quad (44)$$

We can normalize the relation by dividing by V_{spray} the total volume of spray droplets, and we obtain:

$$\sum_{i=1}^{n_c} \frac{M(i, t)}{V_{spray}} = \sum_{i=1}^{n_c} m(i, t) = 1, \quad (45)$$

where we set $m(i, t) = M(i, t)/V_{spray}$. We then have of course, due to mass conservation

$$\frac{d}{dt} \sum_{i=1}^{n_c} m(i, t) = 0. \quad (46)$$

Multiplying by V_i and using the symmetry of $k_c(i, j)$, one obtains the following equation,

$$\frac{\partial m(i, t)}{\partial t} = \sum_{j=1}^{i-1} \tilde{k}_c(i-j, j) m(i-j, t) m(j, t) \\ - m(i, t) \sum_{j=1}^{n_c} \tilde{k}_c(i, j) m(j, t), \quad (47)$$

where we denote $\tilde{k}_c(i, j) = V_{spray} k_c(i, j)/V_j$. We can show that \tilde{k}_c is bounded, knowing $K \propto D^\alpha \exp(-D^\beta)$. Thus we set $K_c^\infty = \sup_{i, j \geq 1} \tilde{k}_c(i, j)$.

In the continuous form, we proceed by multiplying equation Eqn. (27) by V and dividing by $V_{spray} = \int_{V_{min}}^{V_{max}} VN(t) f_n(V, t) dV$ for normalization purpose, and by introducing the mass density function, $M(V, t) = VN(t) f(V, t)$, we obtain, with $g(V, t) = M(V, t)/V_{spray}$, the Mass Flow Formulation, using the symmetry of K_c ,

$$\frac{\partial g}{\partial t}(V, t) = \int_{V_{min}}^V \tilde{K}_c(V - V', V') g(V - V', t) g(V', t) dV' \\ - g(V, t) \int_{V_{min}}^{V_{max}} \tilde{K}_c(V, V') g(V', t) dV', \quad (48)$$

where $\tilde{K}_c(V, V') = V_{spray} K_c(V, V')/V'$, K_c being given by Eqn. (43).

The following condition being by definition assured:

$$\int_{V_{min}}^{V_{max}} g(V, t) dV = 1 \text{ and } \frac{d}{dt} \int_{V_{min}}^{V_{max}} g(V, t) dV = 0. \quad (49)$$

The Monte-Carlo scheme

Once the problem is well-formulated, we look for the drop-size distribution evolution by using the Monte-Carlo scheme. We choose a fixed time step Δt such that $\Delta t K_c^\infty < 1$. We set $t_n = n\Delta t$ and $m_n(i) = m(i, t_n)$. We discretize time by using an explicit Euler scheme for $i \geq 1$,

$$\begin{aligned} \frac{m_{n+1}(i) - m_n(i)}{\Delta t} &= \sum_{j=0}^i \tilde{k}_c(i-j, j) m_n(i-j) m_n(j) \\ &\quad - m_n(i) \sum_{j=1}^{n_c} \tilde{k}_c(i, j) m_n(j). \end{aligned} \quad (50)$$

Thus, we can compute $m_{n+1}(i)$:

$$\begin{aligned} m_{n+1}(i) &= \Delta t \sum_{j=1}^i \tilde{k}_c(i-j, j) m_n(i-j) m_n(j) \\ &\quad - (1 - \Delta t) \sum_{j=1}^{n_c} \tilde{k}_c(i, j) m_n(j) m_n(i). \end{aligned} \quad (51)$$

Using mass conservation of Eqn. (45), we can rewrite Eqn. (51) as:

$$\begin{aligned} m_{n+1}(i) &= \Delta t \sum_{j=1}^i \tilde{k}_c(i-j, j) m_n(i-j) m_n(j) \\ &\quad - \sum_{j=1}^N (1 - \Delta t \tilde{k}_c(i, j)) m_n(j) m_n(i). \end{aligned} \quad (52)$$

We associate to $\{m_n(i) : 1 \leq i \leq n_c\}$, the probability P_n defined on \mathbb{N}^* :

$$P_n = \sum_{i=1}^{n_c} m_n(i) \delta(i). \quad (53)$$

We denote by $(\sigma_A(i))_{i \geq 1}$ the following sequence for a set $A \subset \mathbb{N}^*$:

$$\sigma_A(i) := \begin{cases} 1 & \text{if } i \in A \\ 0 & \text{otherwise} \end{cases} \quad (54)$$

After some algebraic manipulations, we have

$$\begin{aligned} &\sum_{i=1}^{n_c} m_{n+1}(i) \sigma_A(i) \\ &= \sum_{k=1}^{n_c} \sum_{j=1}^{n_c} \{p(i, j) \sigma_A(i+j) + (1-p(i, j)) \sigma_A(i)\} m_n(i) m_n(j). \end{aligned} \quad (55)$$

Here we denote $p(i, j) := \Delta t \tilde{k}_c(i, j)$. The convergent Monte-Carlo scheme is then the following :

we choose N integers, and for all $n \geq 0$, we approximate the solution at time t_n by N particles denoted by $i_{N,n}(1), i_{N,n}(2), \dots, i_{N,n}(N) \in \mathbb{N}^*$ such that,

$$\forall i \quad \frac{1}{N} \sum_{k=1}^N \sigma_{\{i\}}(i_{N,n}(k)) \approx m_n(i). \quad (56)$$

Initialization

To initiate the computation, we choose N numerical particles $i_{N,0}(1), i_{N,0}(2), \dots, i_{N,0}(N) \in \mathbb{N}^*$ such that

$$\frac{1}{N} \sum_{k=1}^N \sigma_{\{i\}}(i_{N,0}(k)) \approx m_0(i). \quad (57)$$

Coalescence

We compute the sizes of particles at time t_{n+1} using the sizes of particles at time t_n . Let $X_{N,n}^1, X_{N,n}^2, \dots, X_{N,n}^N$ be N independent real random variables uniformly distributed in $\{1, 2, \dots, N\}$ and $U_{N,n}^k, 1 \leq k \leq N$ be N independent real random variables uniformly distributed on $[0, 1]$. Let us assume that all the random variables $X_{N,n}^k, 1 \leq k \leq N$ and $U_{N,n}^k, 1 \leq k \leq N$ are independent. The new sizes of particles $i_{N,n+1}(k), 1 \leq k \leq N$ are defined as:

$$\begin{aligned} &i_{N,n+1}(k) \\ &= \begin{cases} i_{N,n}(k) + i_{N,n}(X_{N,n}^k) & \text{if } U_{N,n}^k < p(i_{N,n}(k), i_{N,n}(X_{N,n}^k)) \\ i_{N,n}(k) & \text{otherwise} \end{cases} \end{aligned} \quad (58)$$

It can be shown that this scheme is convergent [17]. It is also to be noted that the approach developed in this paper could easily be extended to other configurations like spray droplets break-up or evaporation, for example.

Application to physically based drop size distribution evolution

The coupling with the previous physical approach from the Maximum Entropy Formalism(MEF) allows our model to be dynamic and sensitive to physical mechanical and operating conditions of the atomizer. Finally, we can deduce a physically-based drop size distribution evolution thanks to our Monte Carlo scheme, using as initialization,

$$m_0(i) = \Delta V g(V_i, 0) = i \Delta V N F_n(i \Delta D) \Delta D / V_{spray}, \quad (59)$$

$$\text{with } V_{spray} = \int_{V_{min}}^{V_{max}} V F_n dV.$$

Finally using Eqn. (59) and with the Monte Carlo scheme Eqn. (58), we solve the evolution of the drop-size distribution of our initial distribution submitted to coalescence effect using the MFA.

MODELING RESULTS

Monte-Carlo scheme convergence and validation

We test the model convergence using $k(i, j) = i + j$, since an analytical solution is known with this kernel. As shown in Fig. 6, a convergence is obtained for a sample of numerical particles of $N = 10000$ and a number of time steps of $P = 400$. The initial condition is

$$f_0^{(i)} = \begin{cases} 1 & \text{if } i = 1 \\ 0 & \text{otherwise} \end{cases} \quad (60)$$

the analytical expression is established in [24]; the second moment is given by:

$$M_2(t) = \sum_{i=1}^N i^2 f(i, t) = e^{2t}. \quad (61)$$

Spray Modeling

We carried out some tests on the evolution of the drop size distribution. We observed that upon time, bigger drops appear in

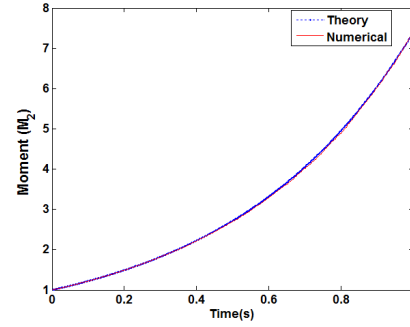


FIGURE 6. Comparison between analytical and numerical solution of second moment.

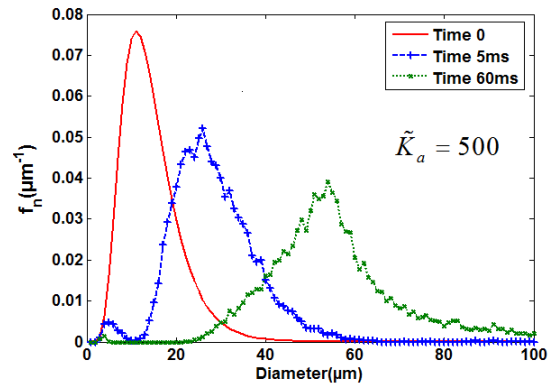


FIGURE 7. Number based drop size distribution, $f_n(D)$, and the coalescence effect.

the spray, as shown in Fig. 7. The first effect of coalescence is observed at the time of 5 ms. At longer times, we observe the coalescence effect, with the emergence of bigger drops shifting by the way the drop size distribution in accordance with experimental measurements involving coalescence. The drop-size distribution presented is bi-modal such an observation has been made on ultrasonic spray², but so far no explanation has been advanced. In [25] for the analysis of ultrasonic atomizer the presence of the second peak near the main peak has been obtained but the second peak is neglected for the MEF distribution fitting. Even though the existence of this supplementary peak is not fully confirmed, based on our model we can retrieve and explain via coalescence such a bimodal distribution in a physical basis.

We show in Fig. 8, the sensitivity study to coalescence effect which leads to physically-based distribution (see Fig. 8(b)). Such a predictive capability and physically-based distribution as in [27] of our model is out of range of classical approach. It is

²Preliminary measurement underway of the SOD shows the same trend far from the nozzle tip.

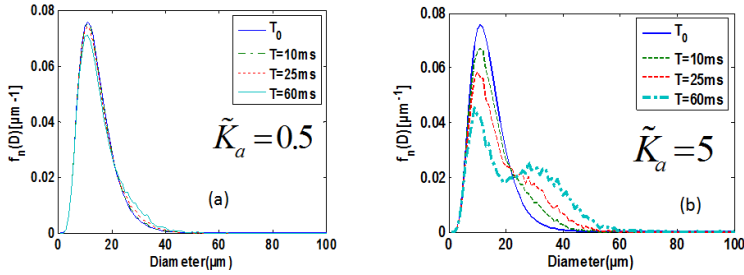


FIGURE 8. Number based drop size distribution, $f_n(D)$ sensitivity to coalescence effect (a) $\tilde{K}_\alpha = 0.5$ and (b) $\tilde{K}_\alpha = 5$.

worth noting that the temporal evolution of the model drop-size distribution could be interpreted as well as the distribution at a spatial point z_s such $z_s = U_s t$, with U_s the spray mean velocity, t being time. Our model could be used as well for CFD modeling as initial condition with a bi-modal (or even multi-modal) distribution in a more physical basis unlike traditional approaches. An improvement of our scheme could be to adopt the Quasi-Monte-Carlo method (QMC) [21].

CONCLUSION

In this paper, we have performed a theoretical study of instantaneous drop size distribution and its temporal evolution applied to a new SOD device. From two visions of the MEF what we call a specific and a general formulation, we derive a new physically-based formulation for spray modeling. With the use of the established Sauter Mean Diameter D_{32} , Volume Mean Diameter D_{30} , and also SOD motion, we have established a physically-based prediction model coupling the three-parameter generalized gamma distribution and conservation laws of MEF. The model parameters have been deduced using a limited set of experimental measurements with the SOD. This new dynamic model is capable of predicting drop size distribution for well specified operating conditions, fluid and channel structure properties. This new approach avoids the traditional adjustment for each operating condition and has better predictive capabilities. The population balance equation, taking into account the interactions between droplets is analyzed. Thus we have established the evolution and resolution of the drop size distribution equation submitted to the coalescence effect. In contrast to Direct Numerical Simulation (DNS), the Mass Flow Algorithm (MFA) we choose allows to preserve the total mass of particles. In this work we consider only binary interactions where two droplets can coalesce to form a bigger one, this before impacting on the substrate. Based on physical hypothesis, we use our proposed coalescence kernel and couple the model with our previous physically-based approach. To solve the problem, a Monte-Carlo Method which is shown to be convergent is developed highlighting the formation

of new drops due to coalescence, leading to a physically based bi-modal distribution.

As future perspective, it is possible to improve the method by adopting quasi-Monte-Carlo simulation method which consists of replacing the (random) Monte-Carlo simulation algorithm by a deterministic one.

REFERENCES

- [1] A.L. Yarin, "Free Liquid Jets and Films: Hydrodynamics and Rheology", *Longman Scientific & Technical and Wiley & Sons*, Harlow, New York, 1993.
- [2] E. Villermaux, "Fragmentation", *Annual Review of Fluid Mechanics* **39**, 419–446, 2007.
- [3] E. Villermaux, P. Marmottant, and J. Duplat, "Ligament-Mediated Spray Formation", *Phys. Rev. Lett.* **92**, 074501, 2004.
- [4] E. Babinski and P. E. Sojka, "Modeling drop size distributions", *Progress in Energy and Combustion Science*, **28**, 303–329, 2002.
- [5] H. Liu, "Science and Engineering of Droplets - Fundamentals and Applications", *William Andrew Publishing-Noyes*, 2000.
- [6] C. Dumouchel "The Maximum Entropy Formalism and the Prediction of Liquid Spray Drop-Size Distribution" *Entropy*, **11**, 713-747, 2009.
- [7] X. Li and R.S Tankin , "Derivation of droplet size distribution in sprays by using information theory", *Comb. Sci. Technol.*, **60**, 345–357, 1988.
- [8] C. Dumouchel, "A New Formulation of the Maximum Entropy Formalism To Model Liquid Spray Drop-Size Distribution", *Part. Part. Syst. Charact.*, **23**, 468–479, 2006.
- [9] J.H. Lienhard, P.L.Meyer, "A physical basis for the generalized gamma distribution", *Quart. Applied Math.*, **25**, 330–334, 1967.
- [10] J. Cousin, S. J. Yoon, C. Dumouchel, "Coupling of Classical Linear Theory and Maximum Entropy Formalism for Prediction of Drop-Size Distribution in Sprays: Application to Pressure Swirl Atomizers". *Atomization and Sprays*, **6**, 601–622, 1996.
- [11] M. Tembely, C. Lécot and A. Soucemarianadin, "Generation of a spray on demand using a vibrating micro-channel", *Proc. of the 1st European Conf. on Microfluidics*, 2008.
- [12] M. Tembely, C. Lécot and A. Soucemarianadin, "Theoretical and Experimental Fluid/Structure Investigation of an On Demand Induced Spray", *Proc. of the 11th Triennial Internat. Ann. Conf. on Liquid Atomization and Spray System*, ICLASS, Colorado USA, 2009.
- [13] S. Chapman and T.G. Cowling. "The Mathematical Theory of Non-Uniform Gases", *Cambridge University Press*, Cambridge, 1970.

- [14] G. Kocamustafaogullari and M. Ishii, "Foundation of the interfacial area transport equation and its closure relations", *Int. J. Heat Mass*, **38**, 481–493, 1995.
- [15] A.K. Chesters and G. Hoffman, "Bubble coalescence in pure liquids", *Appl. Sci. Res.*, **38**, 353–361, 1982.
- [16] V. G. Levich, "Physicochemical Hydrodynamics", *Prentice-Hall*, Englewood Cliffs, 1962.
- [17] M. Tembely, "Atomisation Induite par Interaction-Fluide Structure", PhD, Grenoble Univseristé, 2010.
- [18] C. Lécot and A. Tarhini, "A quasi-stochastic simulation of the general dynamics equation for aerosols", *Monte Carlo Methods Appl.*, **13**, 369–388, 2007.
- [19] N. Fdida, "Développement d'un système de granulométrie par imagerie. Application aux sprays larges et hétérogènes", PhD Thesis, Coria, 2008.
- [20] J.B. Blaisot and J. Yon, "Droplet size and morphology characterization for dense sprays by image processing: application to the Diesel spray", *Experiments in Fluids*, **39**, 977–994, 2005.
- [21] C. Lécot and W. Wagner, "A quasi-Monte Carlo scheme for Smoluchowski's coagulation equation", *Math. Comput.*, **73**, 2004.
- [22] H. Babovsky, "On a Monte Carlo scheme for Smoluchowski's coagulation equation", *Monte Carlo Methods Appl.*, **5**, 1–18, 1999.
- [23] R.J. Lang, "Ultrasonic atomisation of liquids". *J. Acoust. Soc. Am.* **34**, 6-8, 1962.
- [24] A. Golovin, "The solution of the coagulating equation for cloud droplets in a rising air current", *Izv. Geophys. Ser.*, **5**, 482–487, 1963.
- [25] C. Dumouchel, D. Sindayihebura and L. Bolle, "Application of the Maximum Entropy Formalism on Sprays Produced by Ultrasonic Atomizers", *Part. Part. Syst. Charact.*, **20**, 150–161, 2003.
- [26] M. Lecompte and C. Dumouchel "On the Capability of the Generalized Gamma Function to Represent Spray Drop-Size Distribution", *Part. Part. Syst. Charact.*, **25**, 154 – 167, 2008.
- [27] G. Brenn, St. Kalenderski and I. Ivanov "Investigation of the stochastic collisions of drops produced by Rayleigh breakup of two laminar liquid jets", *Phys. Fluids* **9**, 349, 1997.